



21st IAEA Fusion Energy Conference, Chengdu, China, 2006

Overview of Physics Results from MAST

**Brian Lloyd for the MAST Team
Euratom/UKAEA Fusion Association**

*This work was jointly funded by the UK Engineering & Physical
Sciences Research Council and Euratom*

UKAEA





Outline

- Introduction – technical highlights
- Confinement & transport (inc. pellet injection)
- Heating and current drive - NBI, EBW
- Stability studies – locked modes, sawteeth, fast particle instabilities
- Edge physics – ELM & pedestal studies, L-mode turbulence, disruptions
- Summary

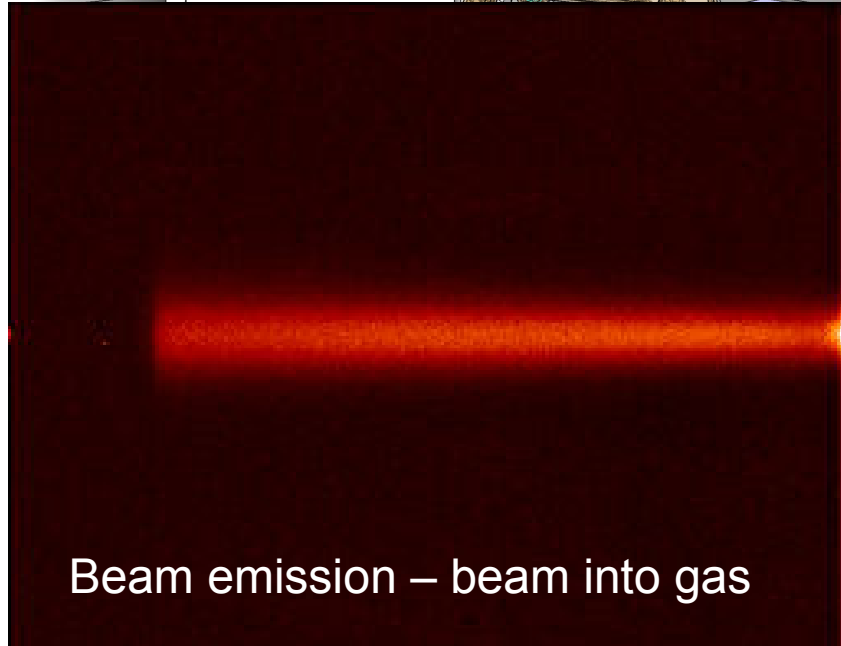
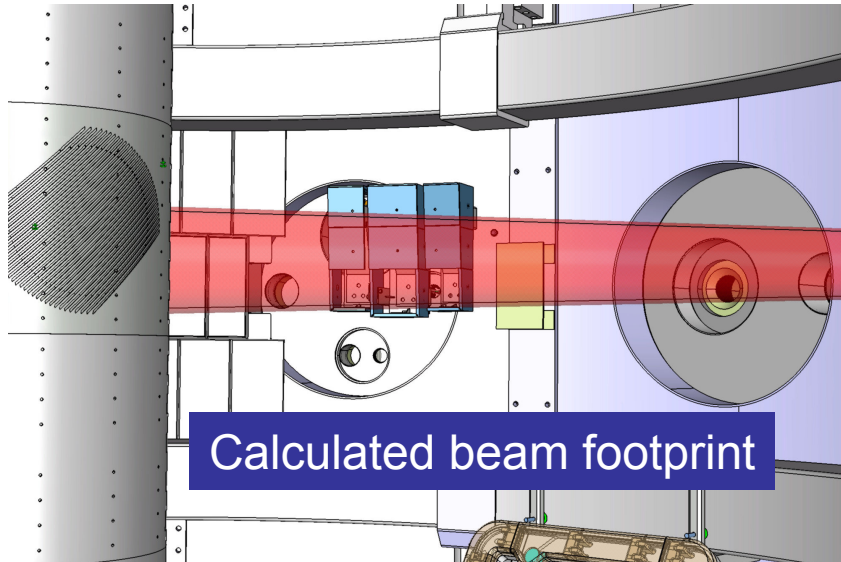


MAST Technical Highlights

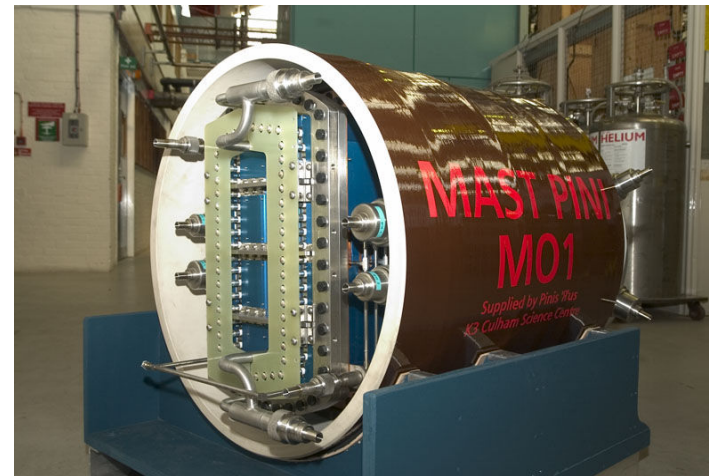
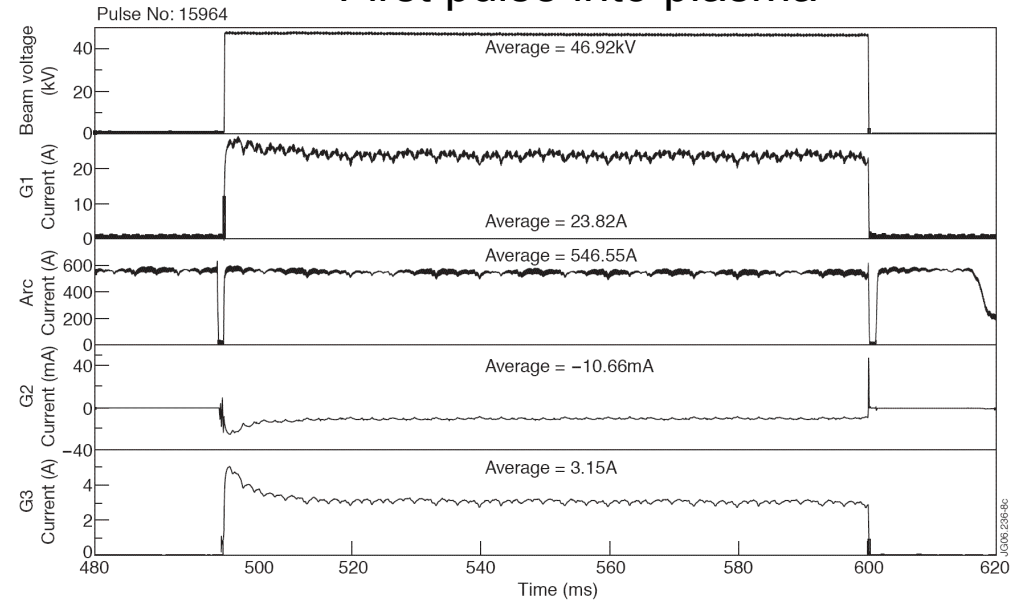
- ❑ First operation of new long pulse NBI source (JET-style PINI 2.5MW/5s) into plasma
- ❑ First deployment of real time equilibrium construction in digital control system – based on RTEFIT and PCS (General Atomics)
- ❑ First data from prototype MSE system (in collaboration with KTH Sweden)
- ❑ Implementation of new edge Thomson scattering system – used to measure evolution of pedestal & near SOL down to $1 \times 10^{18} \text{m}^{-3}$, 5eV with 1cm/5 μs resolution
- ❑ CXRS measurements of rotation/ion temperature on the scale length of the ion Larmor radius with 5ms resolution
- ❑ Implementation of improved imaging diagnostics allowing, for example, measurement of filamentary structures at the plasma edge with 10 μs resolution



First PINI operational

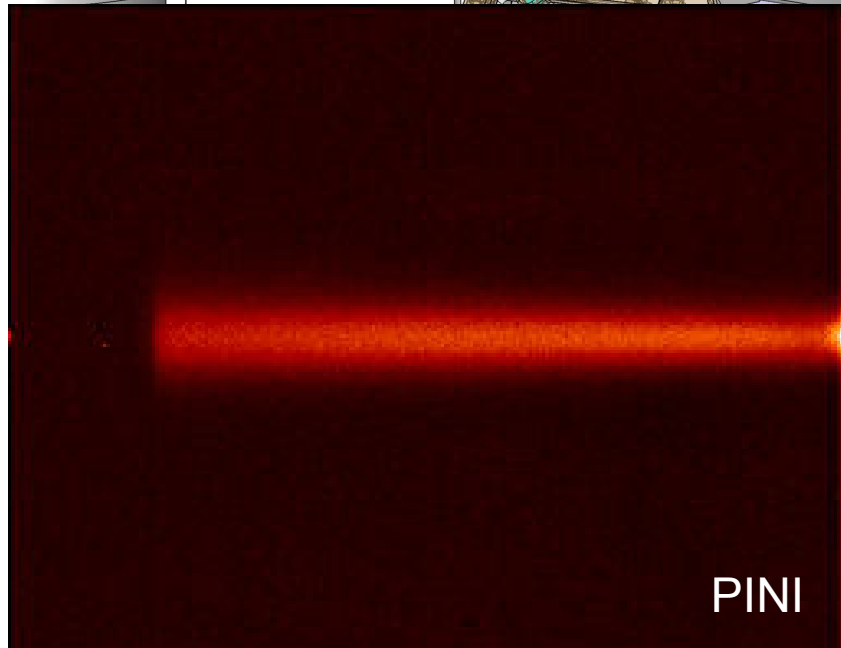
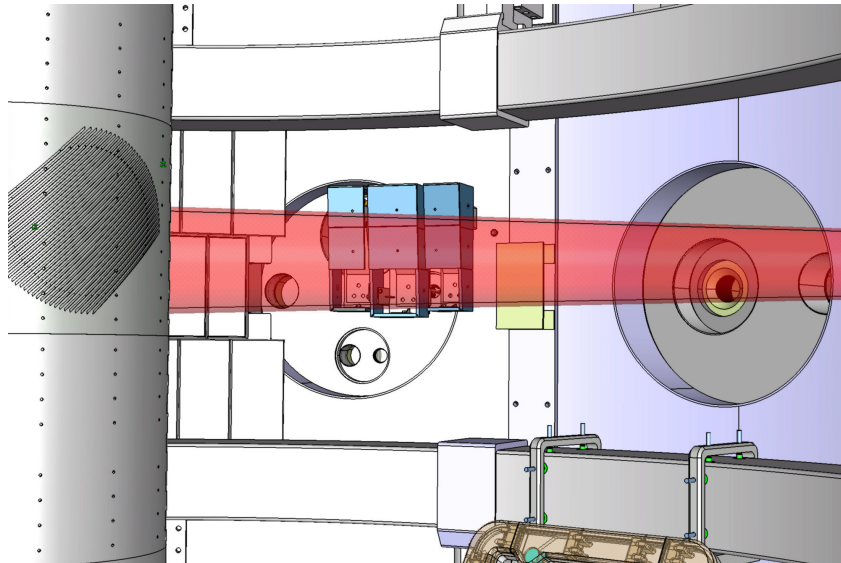


First pulse into plasma

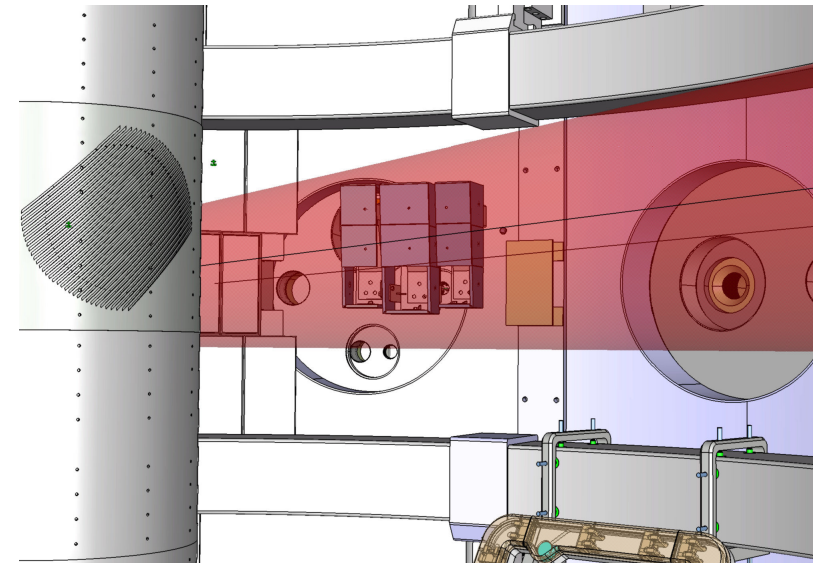




PINI versus Duopigatron



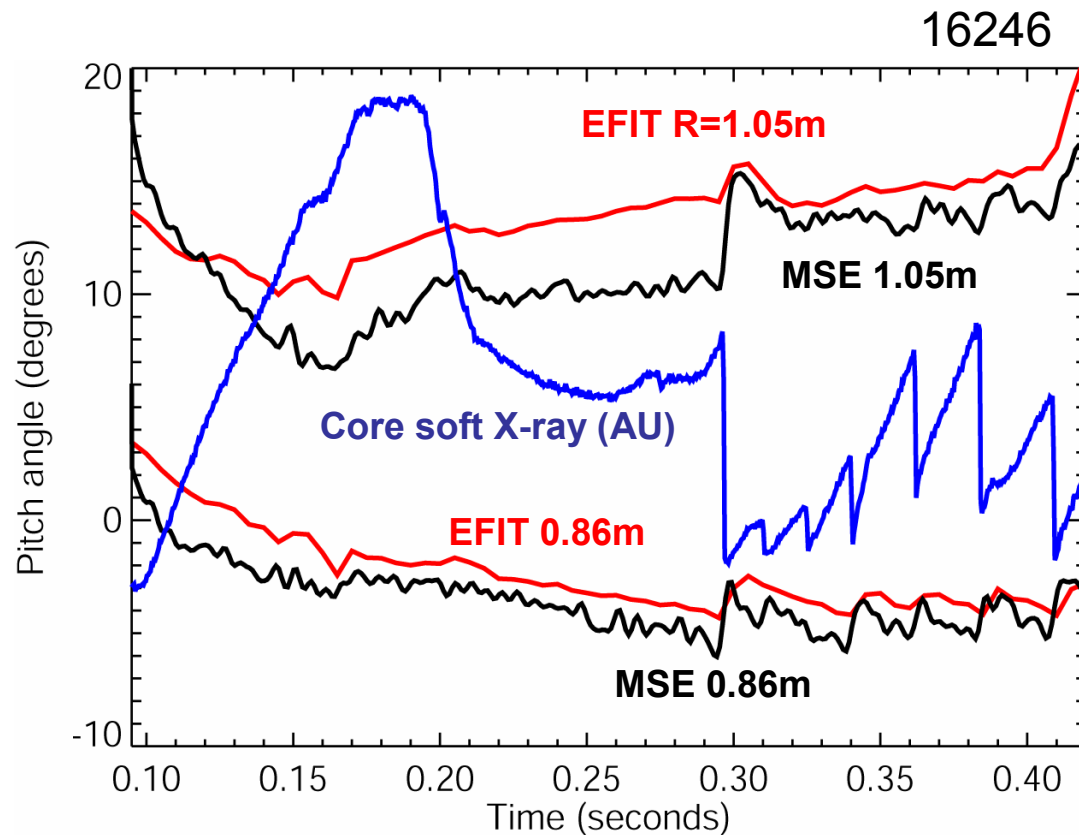
PINI



DUOPIGATRON



PILOT MSE measurements



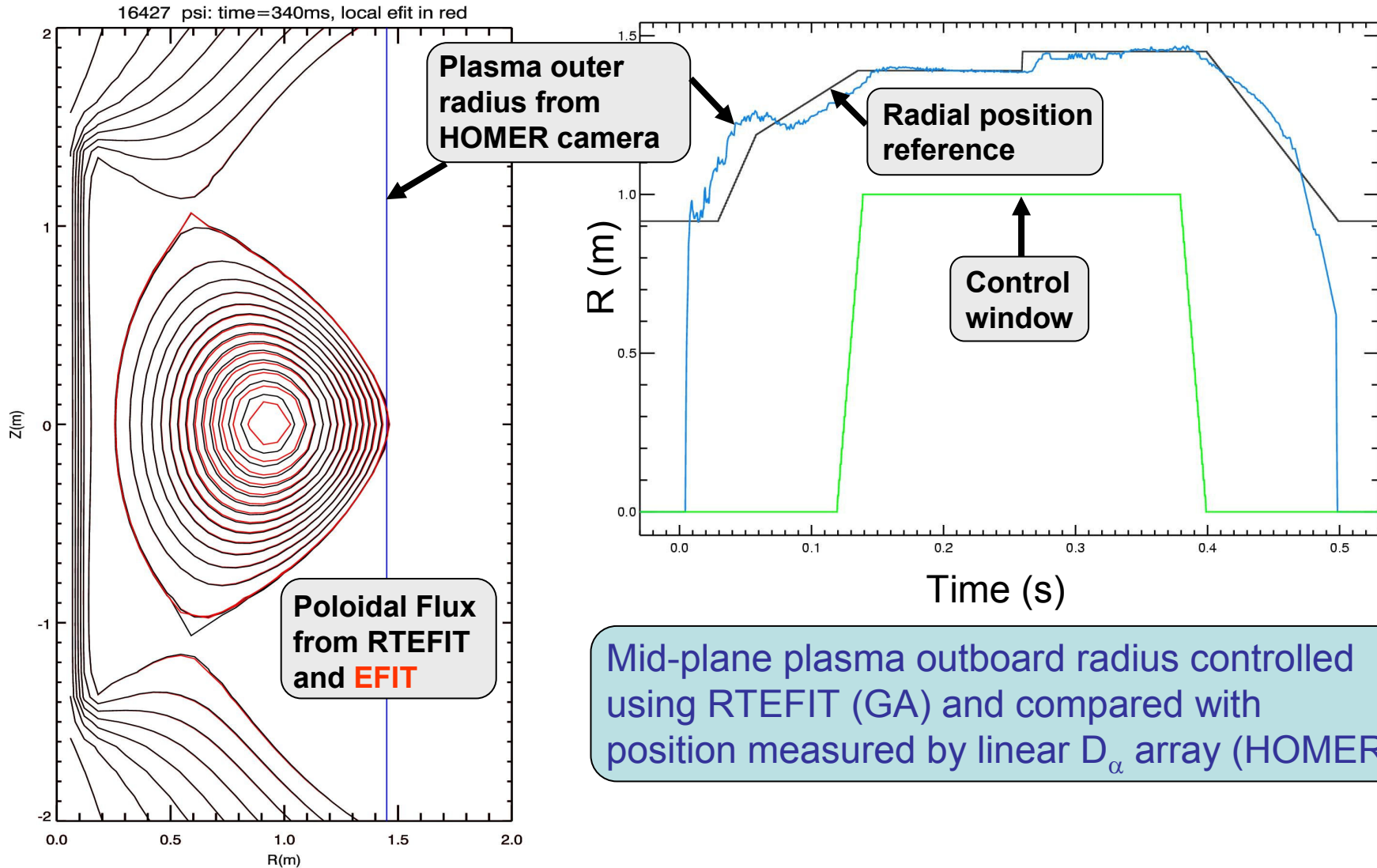
Results from two-chord pilot system (in collaboration with KTH Sweden)

Readily expandable to multi-channel system for full q-profile.

5ms resolution



RTEFIT radial position control

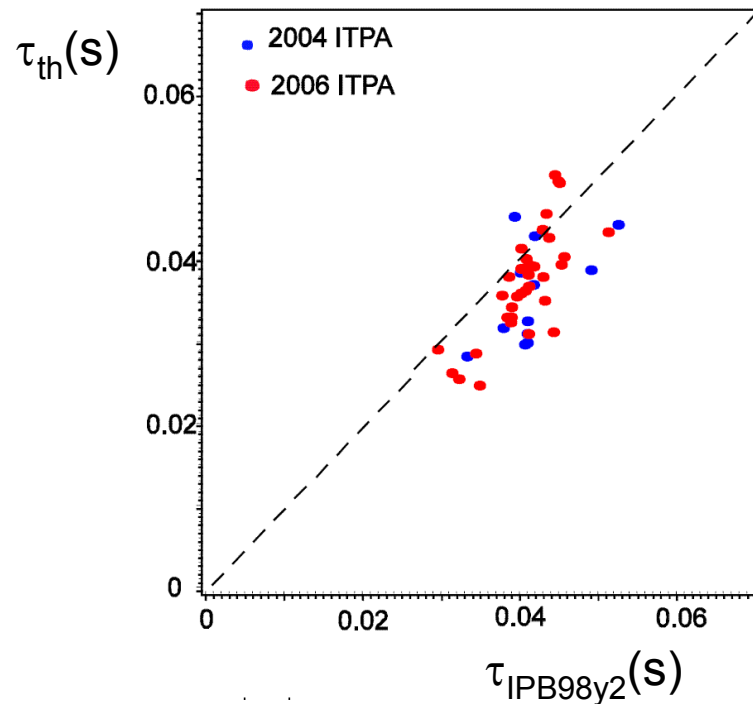


NB. Radial position normally controlled via HOMER, rather than magnetic measurements in MAST



Confinement scaling

MAST confinement database (L-mode & H-mode) extended to higher I_p (1.2MA),
- also includes discharges fuelled by deuterium pellets



Increased submissions (x4) of MAST data to ITPA H-mode confinement database
- broadly agree with IPB98y2

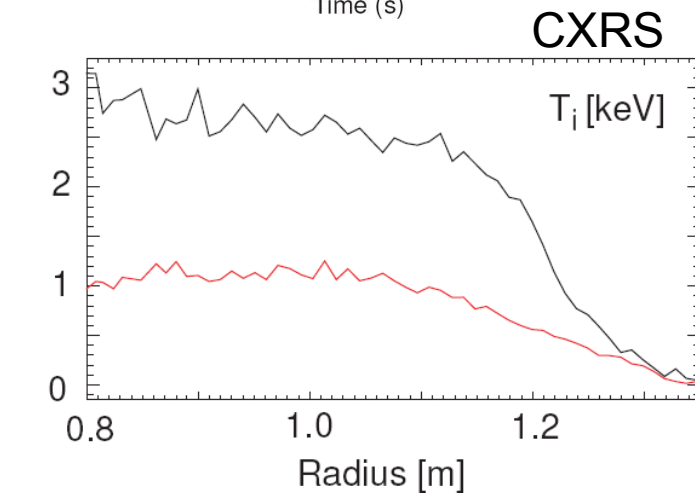
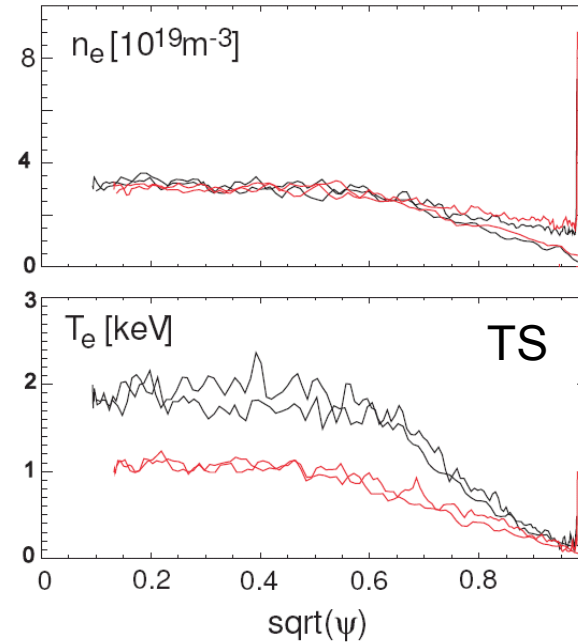
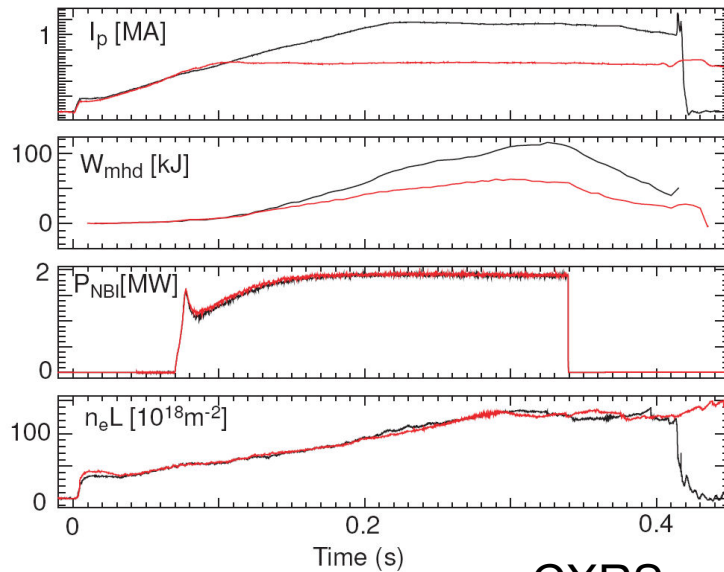
L-mode scaling L97 underestimates confinement in MAST L-mode
- suggests a more positive dependence on ϵ than given by scaling



Confinement: I_p scaling

I_p scaling in L-mode

- x2 I_p scan (0.6 – 1.2MA)
- excellent P_{NBI} & n_e match



$$\tau_E^{\text{th}} \propto I_p, \text{ close to L97 scaling } (\tau_E^{\text{th}} \propto I_p^{0.96})$$

1.2MA H-mode operation recently established
- I_p scaling in H-mode being evaluated



Confinement: β - ε scaling

β - ε interplay in H-mode

Correlation between β and ε introduces a strong interplay between the β and ε scalings derived from database analysis

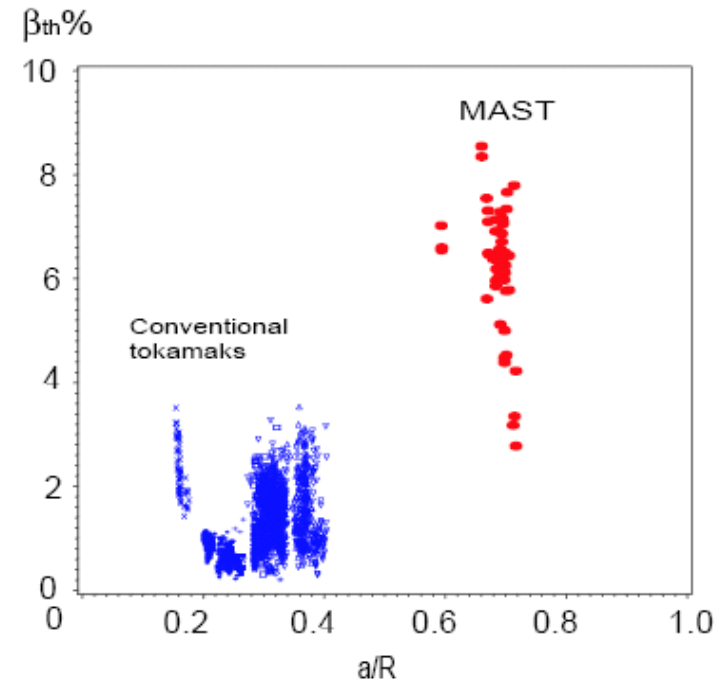
For gyro-Bohm scaling with β degradation as in IPB98(y,2):

$$B\tau_E \propto \rho_*^{-3} \beta^{-1} \varepsilon^{0.77 \pm 0.3}$$

For gyro-Bohm with β independence:

$$B\tau_E \propto \rho_*^{-3} \beta^0 \varepsilon^{-0.63 \pm 0.2}$$

[M. Valovic et al, Nuc. Fus. 45 (2005) 942, S. Kaye et al, PPCF 48 (2006) A429]

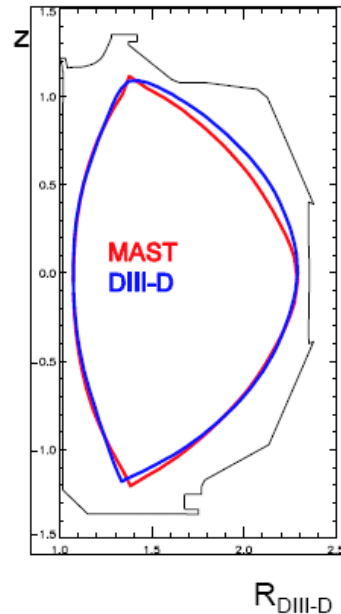




Confinement: β - ε scaling

β - ε interplay in H-mode

MAST 8414 DIII-D 122815



MAST-DIII-D comparison

$$B \tau_{Eth} \propto \rho_*^{x_\rho} \beta^{x_\beta} v_*^{x_v} \varepsilon^{x_\varepsilon} M^{x_M} q^{x_q} K^{x_K}$$

Matching plasma shape, poloidal ρ_p^* , β_p and an/T^2 provides a constraint on the exponents in the power law scaling:

$$-2.92 = 0.95x_\rho + 1.57x_\beta - 2.56x_v + x_\varepsilon$$

(MAST cross-section displaced in R)

Constraint is consistent with:

- gyro-Bohm Scaling ($x_\rho = -3$)
- weakly favourable collisionality scaling (as observed in MAST & other devices)
- β - ε interplay in accord with that derived from the database analysis

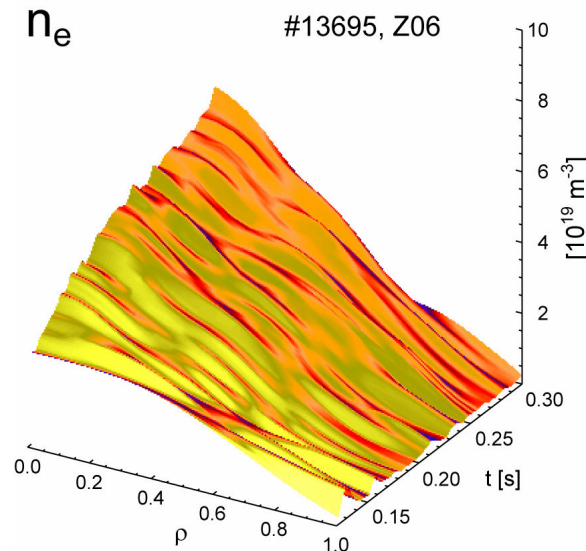
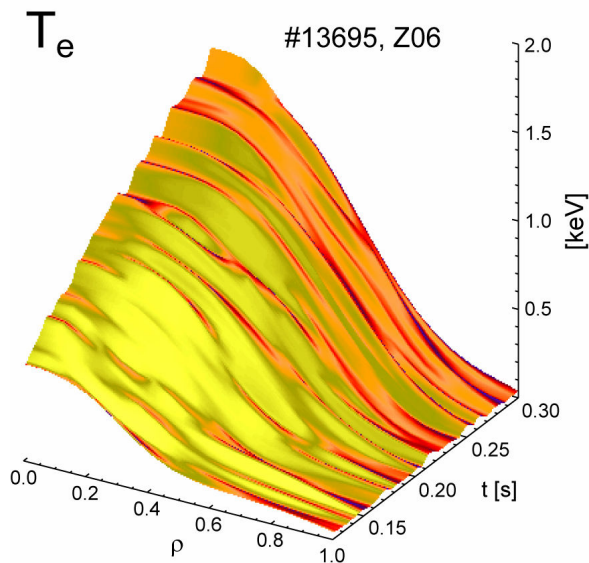
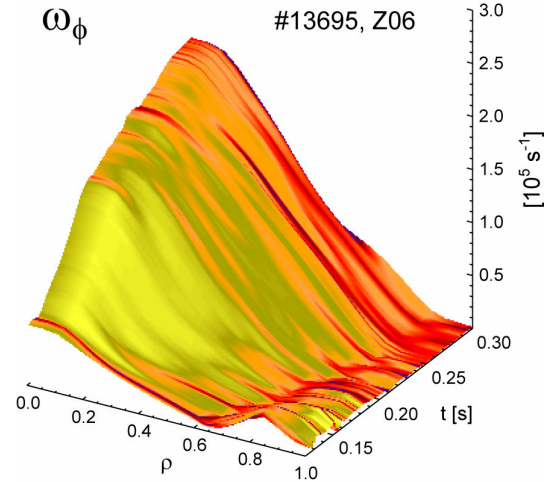
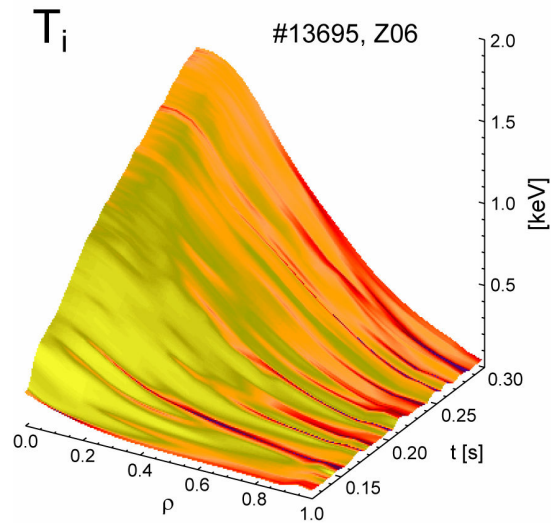
DIII-D data provided by C. Petty (GA)

UKAEA





High resolution kinetic measurements



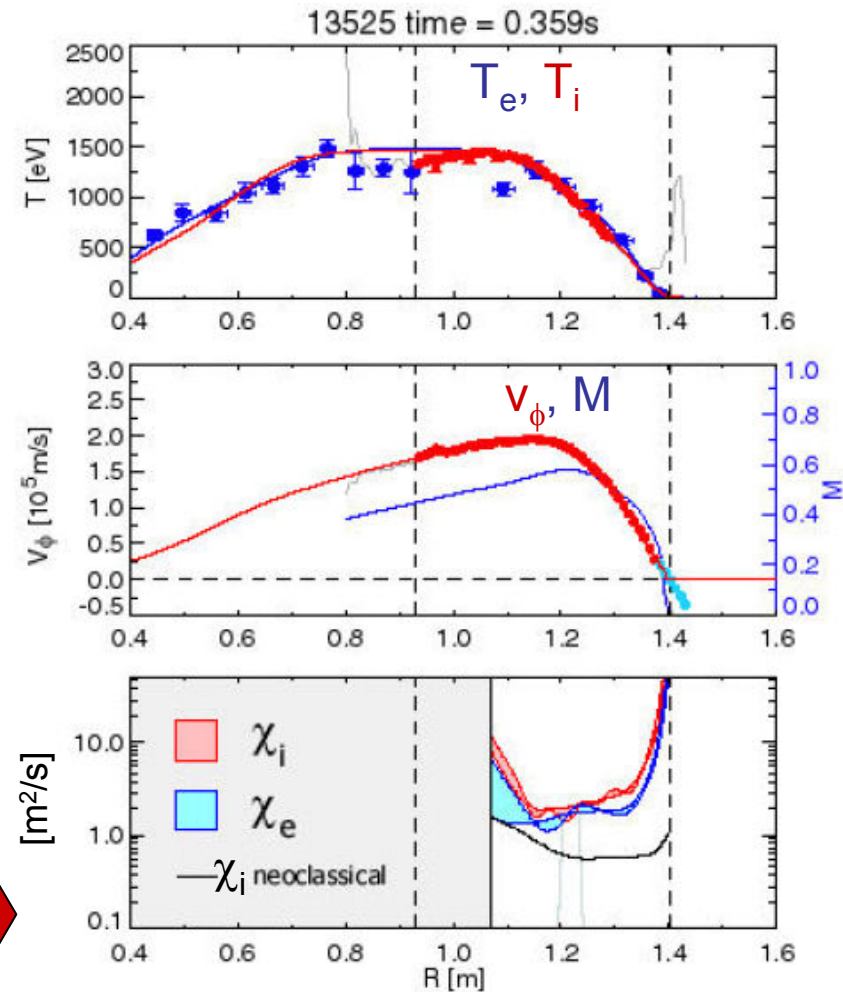
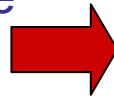
High resolution time-resolved (5ms) CXRS and Thomson scattering allow detailed transport analysis e.g. using TRANSP



Transport analysis

High ExB flow shear in MAST

- ITBs readily formed in both electron and ion channel
- χ_e, χ_i can approach χ_i^{neo} at ITB and in H-mode
- For both co- and counter-NBI, barriers form in the core initially then broaden substantially and weaken
- Broad rotation profile with counter-NBI gives $\chi_e \sim \chi_i \sim 2\text{m}^2/\text{s}$ over a wide region [R. Akers et al, EX/P3-13]



Underlying physics being explored with GS2, CUTIE – non-linear GS2 calculations give electron thermal diffusivity close to experimental values

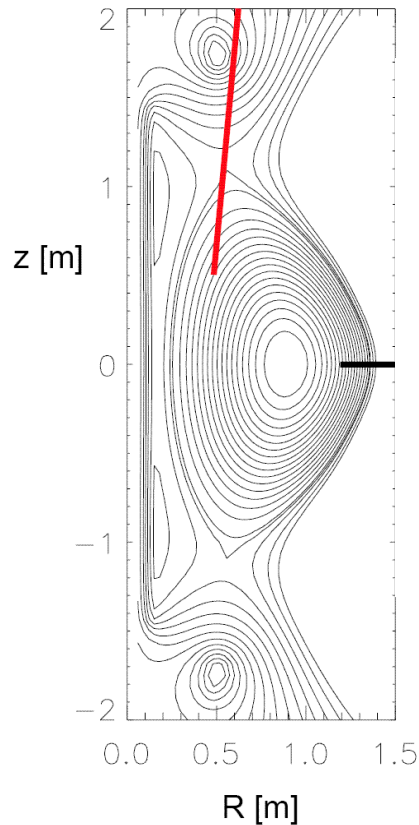
[J. Connor et al, TH/P2-2]



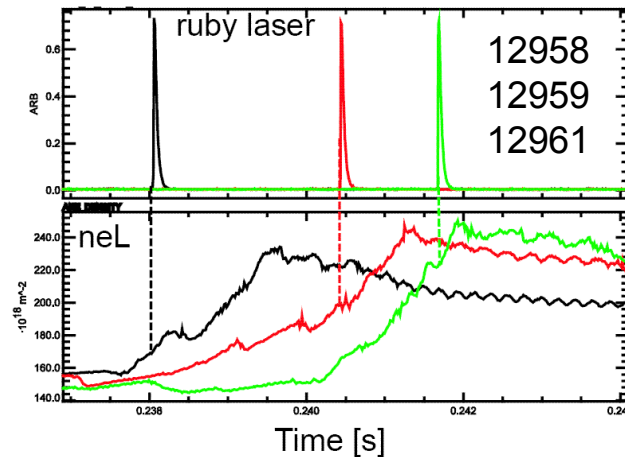
Pellet injection

Top/inboard and mid-plane/outboard launch (≤ 6 pellets/pulse)

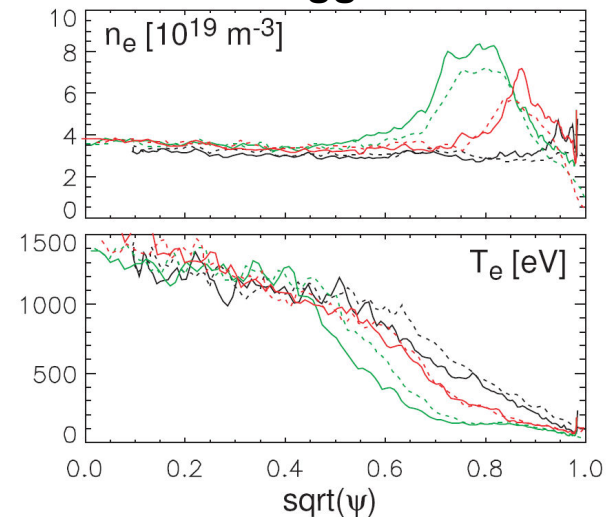
Profile evolution during pellet ablation:



Top launch, 380 m/s, H-mode with NBI



Pellet-triggered TS



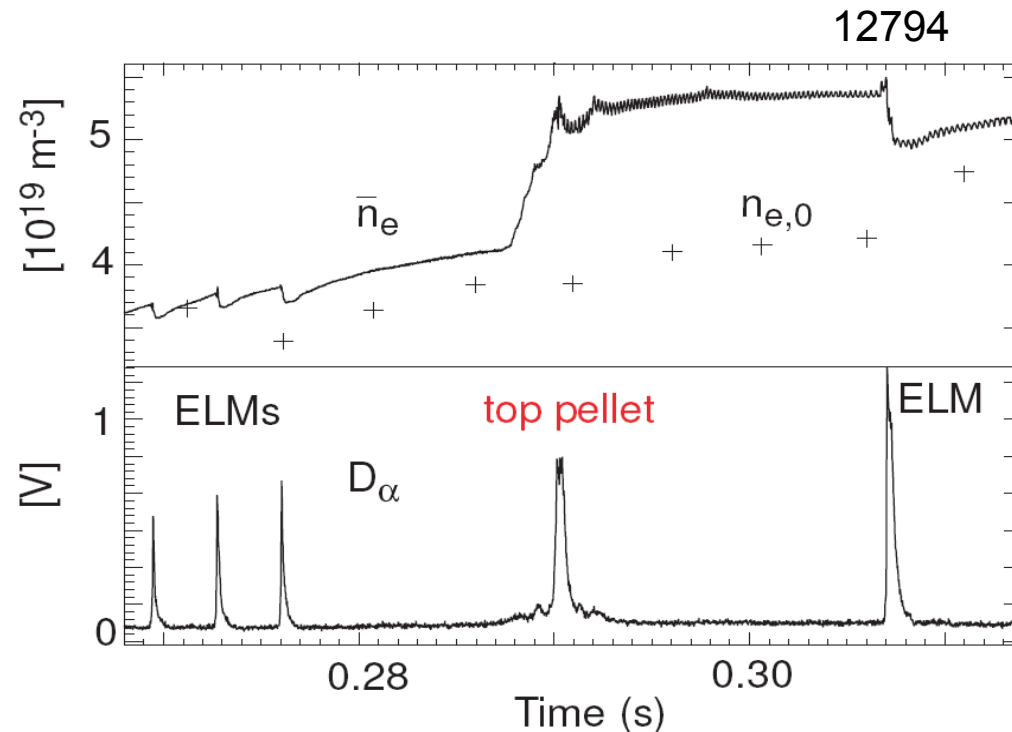
Pellet deposition zone develops inside pedestal ($r_{\text{pellet}}/a \sim 0.75$) with positive density gradient and temperature depression as expected in ITER.

Pellet ablation modelled by various codes – post-pellet profiles can be well-produced by neutral gas shielding model but not always the case. On-going analysis to understand better the ablation process & the role of drifts.



Pellet injection into H-mode

Shallow pellet injection into NBI-heated H-mode does not necessarily trigger an ELM or an H→L transition



Confinement penalty $\sim 10\%$ associated with pellet injection (cf. JET)

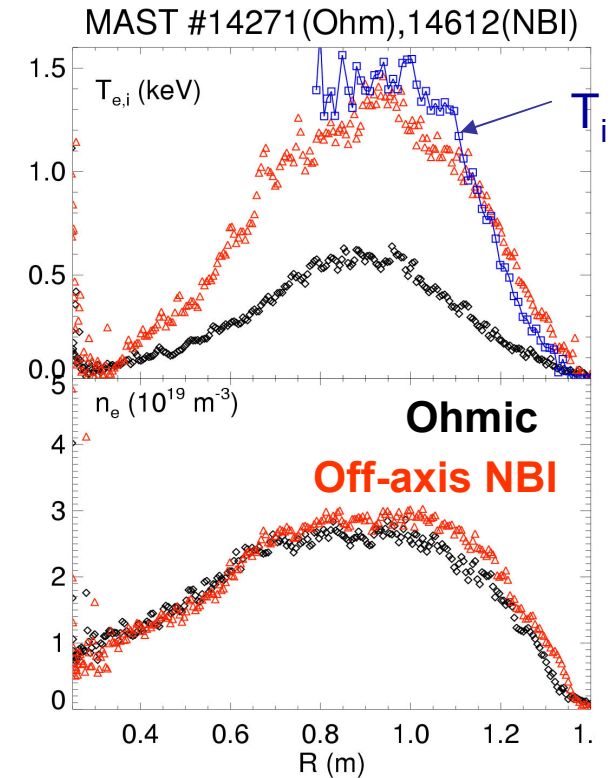
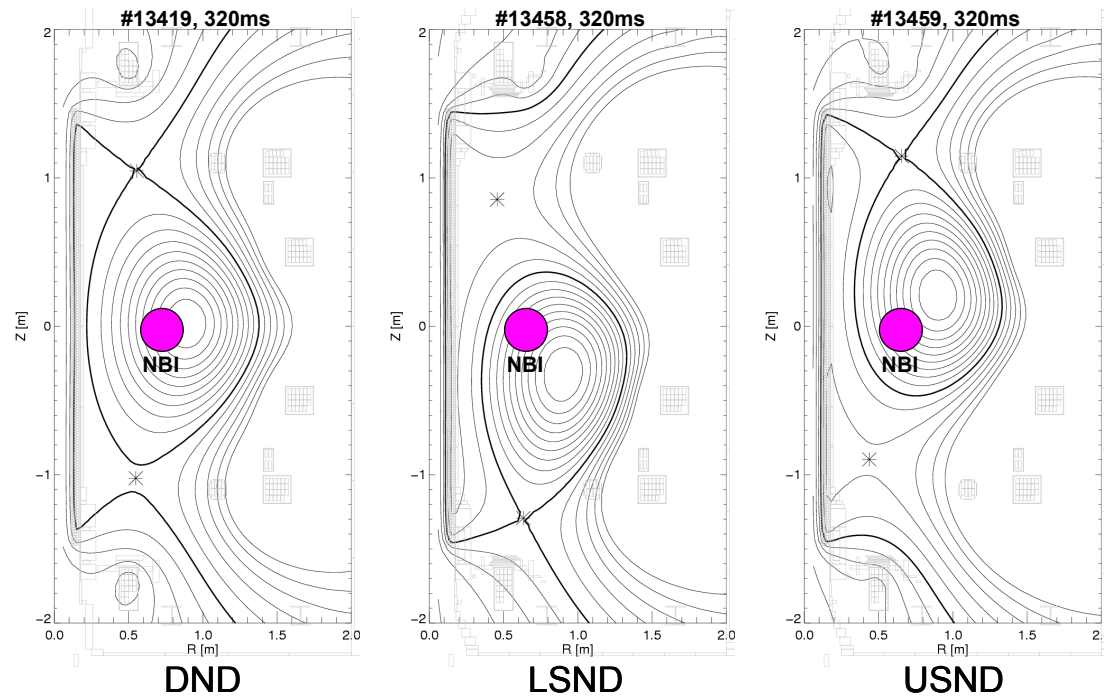
$$\Delta H_{\text{pellet}} = \bar{H}_{\text{pellet}} - \bar{H}_{\text{w/o pellet}} = -0.10 \pm 0.05$$



Off-axis NBI

Large MAST vessel allows exploratory studies of off-axis NB heating & current drive in vertically displaced SND plasmas

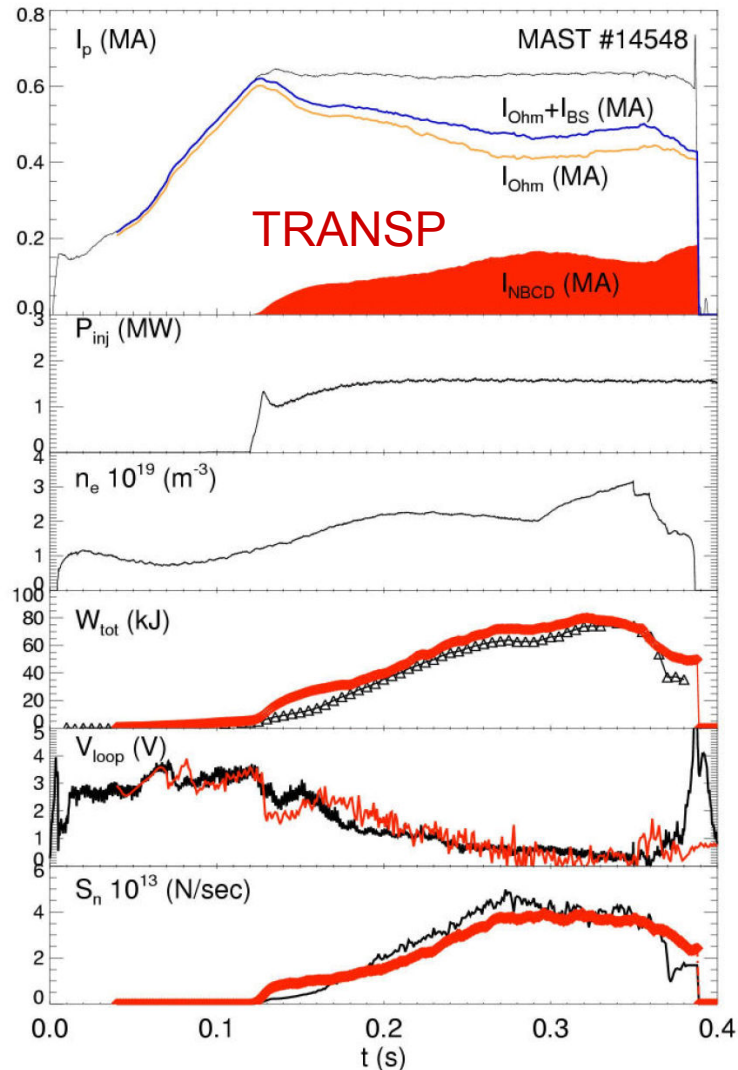
Efficient off-axis heating observed – comparable to on-axis heating



[R. Akers et al, EX/P3-13]



Off-axis NBCD



[R. Akers et al, EX/P3-13]

TRANSP analysis gives good fit to experimental data & indicates $I_{NBCD}/I_p \sim 25\%$

Measurements ($q=1$ appearance, I_j) indicate larger off-axis driven current for LSND compared to USND – as predicted by theory.

B_θ/B_ϕ not small in MAST – results in higher trapped ion population for USND (confirmed by NPA measurements) – effect negligible at conventional aspect ratio

Experiments will be repeated at higher P_{NBI} & with MSE to confirm off-axis driven current

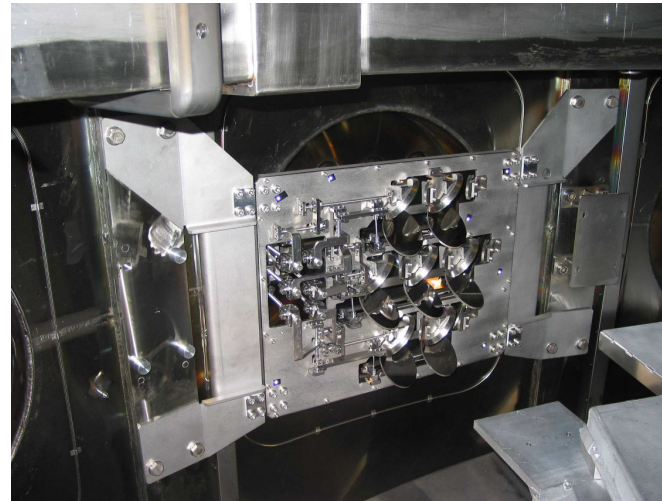


Electron Bernstein Waves (EBW)

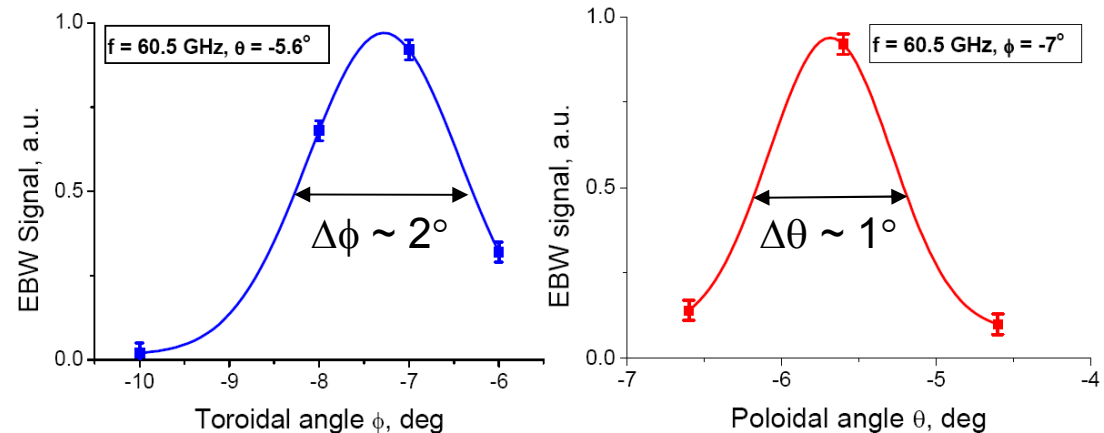
Proof-of-principle tests of O-X-B heating scheme at 60 GHz

Narrow mode conversion 'window'

Launcher allows independent control of θ , ϕ , polarisation for up to 7 beams



EBW emission used to measure mode conversion window and optimise antenna/target plasma parameters



[V. Shevchenko et al, EX/P6-22]

High density Ohmic H-mode target

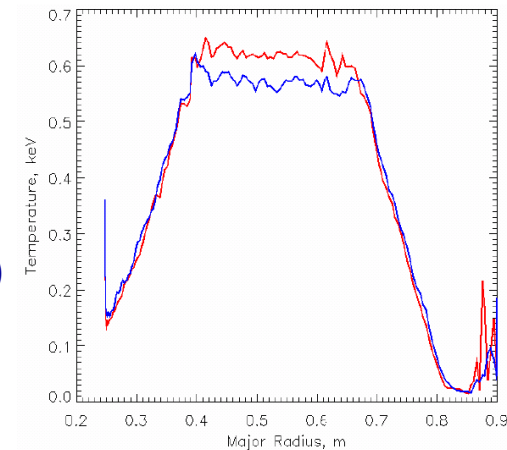


EBW heating results

High density Ohmic H-mode

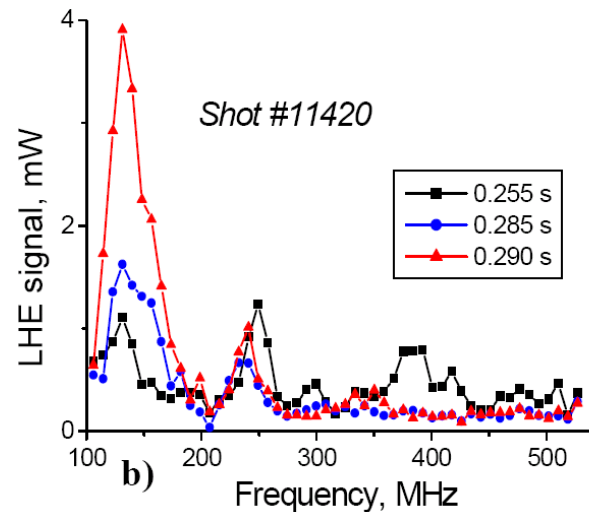
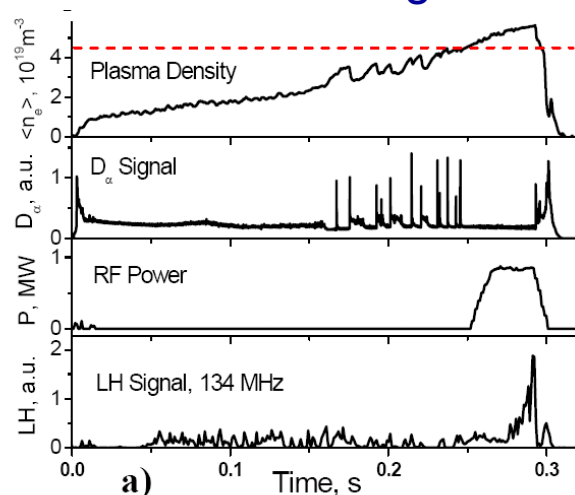
- core absorption possible but very narrow conversion window
- after careful antenna alignment a 10% increase in T_e was observed ($P_{EBW} \sim 0.4\text{MW}$)

T_e profiles (TS)



ELM-free H-mode

- only peripheral absorption possible
- parametric decay waves (subject to $\sim 80\text{ kW}$ RF power threshold) indicate significant mode conversion efficiency ($>50\%$)

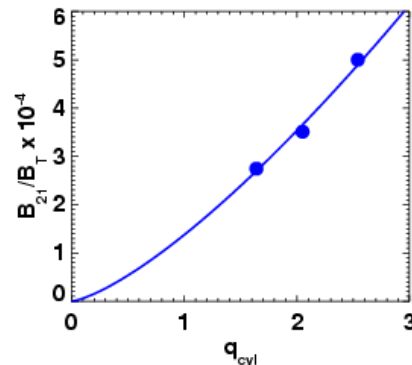
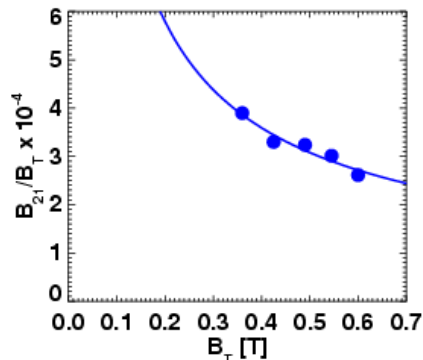
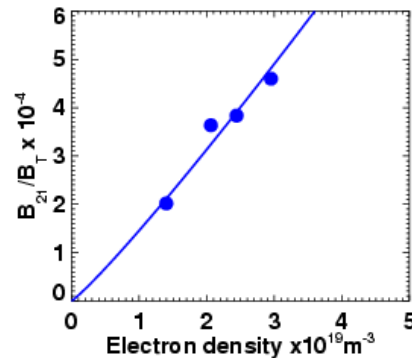
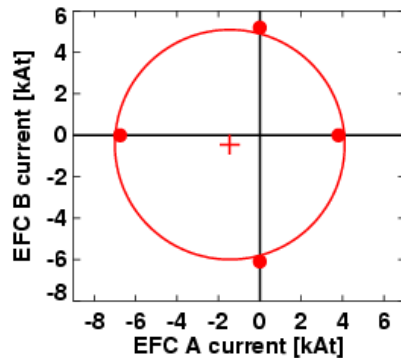




Locked mode threshold scaling

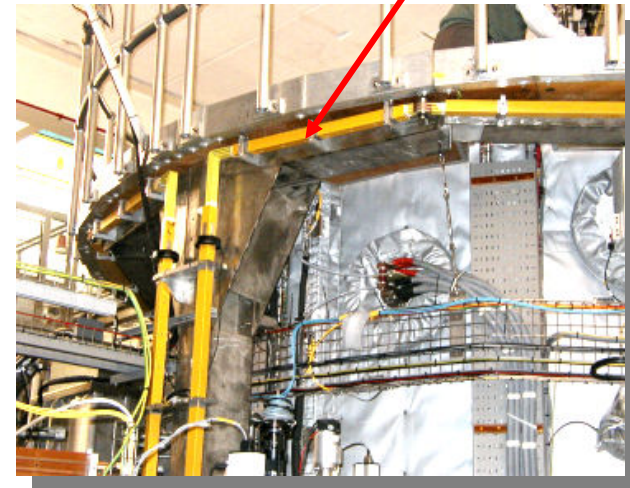
- Similar to that in conventional aspect ratio tokamaks

$$\frac{B_{21}}{B_T} \propto n_e^{1.1 \pm 0.2} B_T^{-0.7 \pm 0.1} q_{cyl}^{1.4 \pm 0.2}$$



MAST-DIII-D comparison shows aspect ratio scaling weak [D. Howell et al, APS 2004]

Error field coils



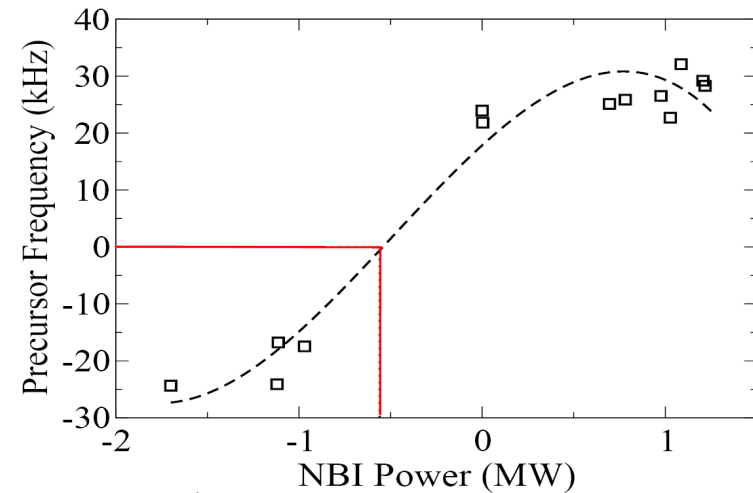
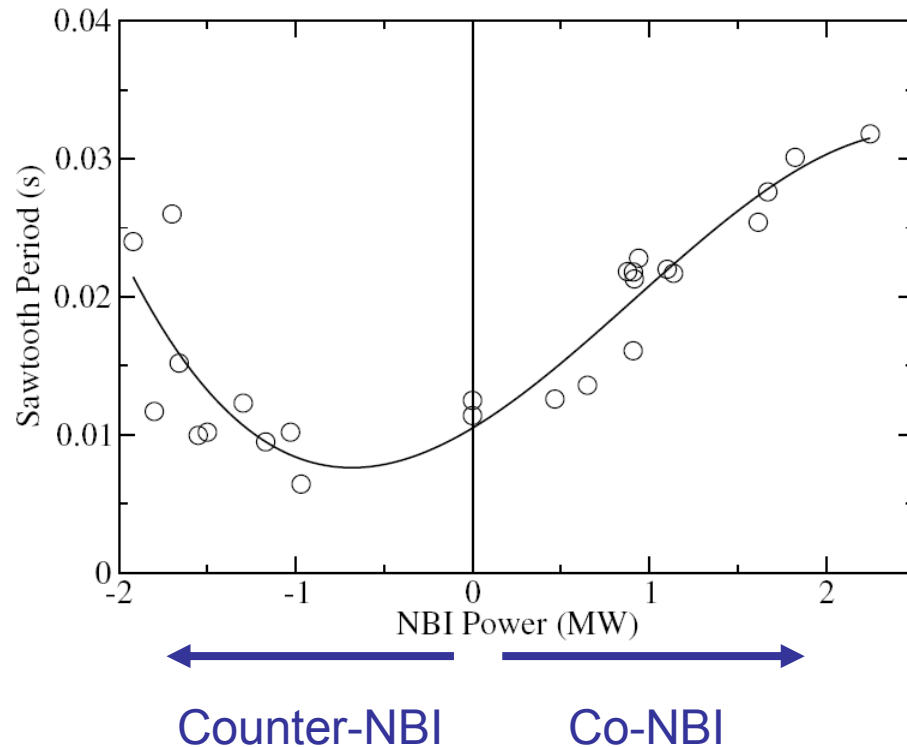
By applying an $n=1$ field at four toroidal phases we can obtain simultaneously the error field correcting currents and the locked mode threshold.

[S. Pinches et al, EX/7-2Ra]



Sawtooth stabilisation by rotation

High toroidal flows in the ST can stabilise the $n=1$ internal kink mode



[-ve frequency \Rightarrow mode rotation in counter- I_p direction]

Minimum τ_{st} when $f_{precursor} = 0 \Rightarrow$ NBI-induced rotation balances intrinsic rotation of mode at the ion diamagnetic frequency

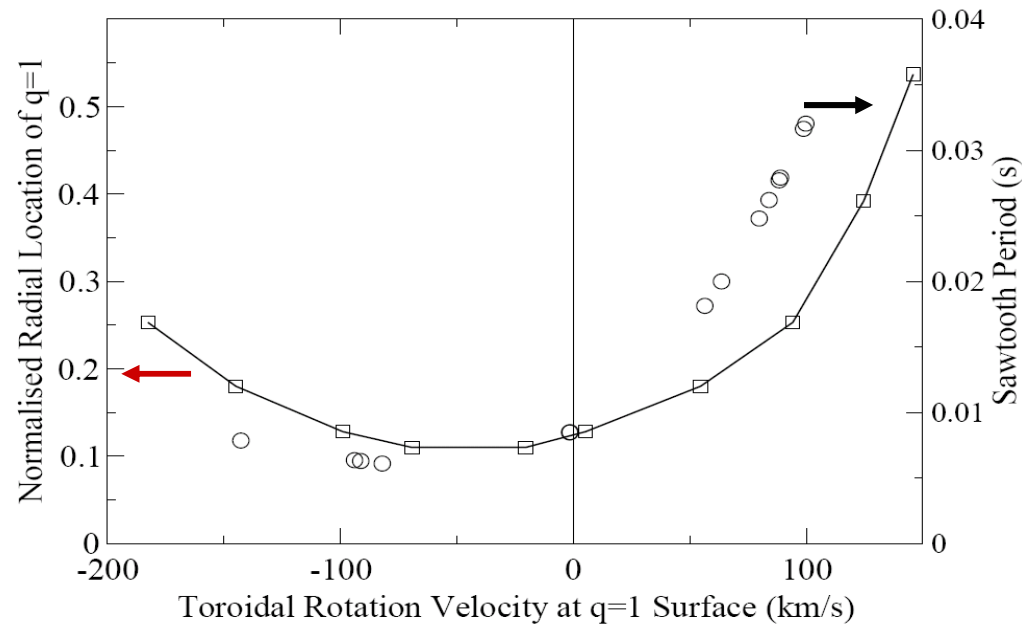


Sawtooth stabilisation - theory

MISHKA-F: stability of ideal internal kink mode ($n=1$) with respect to toroidal rotation, at finite ion diamagnetic frequency

- Minimum τ_{st} agrees with minimum marginally stable $q=1$ radius

Radial location of marginally stable $q=1$ surface

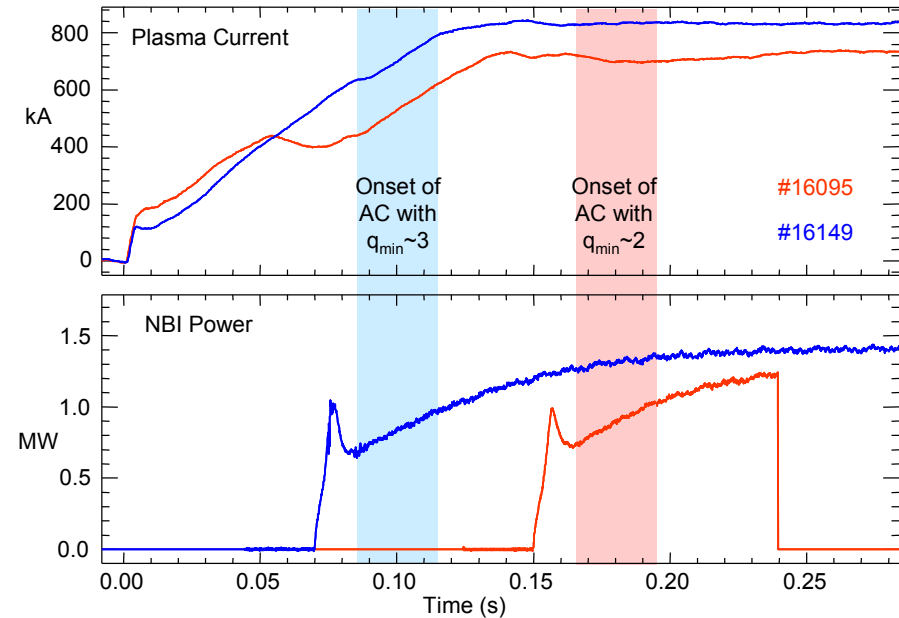
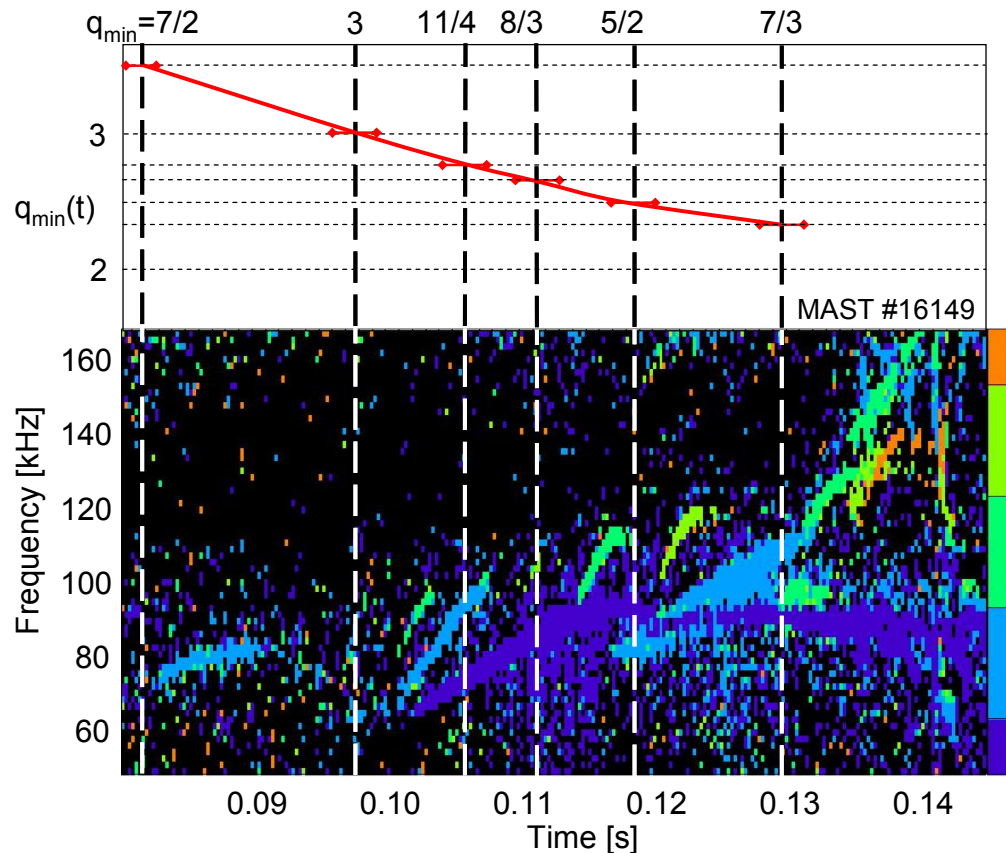


Computations show that stabilisation is determined by magnitude of rotation at $q=1$ rather than flow shear. Role of kinetic effects under investigation.



Alfvén Cascades (ACs)

A wide range of fast particle instabilities is observed in MAST (TAEs, EAEs, chirping modes, fishbone instabilities) – strong chirping activity prevents observation of ACs at high power.



At low power (typically < 1.5MW) ACs observed in two regimes

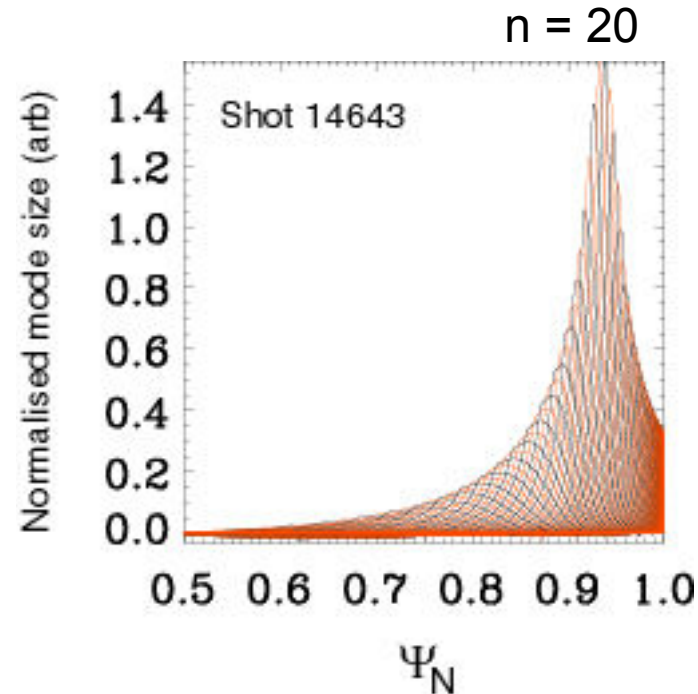
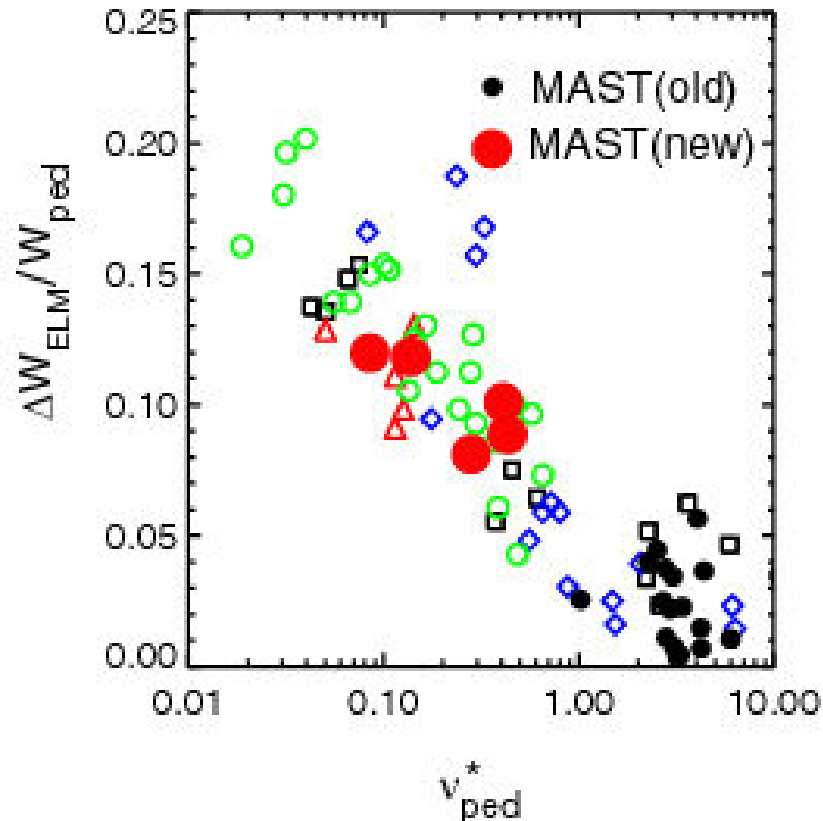
[S. Pinches et al, EX/7-2Ra]



ELM & pedestal physics

MAST database now extended to high $T_{e\text{ped}} (\leq 435\text{eV})$, low v_{ped}^* (~ 0.08) plasmas

□ ASDEX-U ♦ DIII-D ▲ JT-60U ○ JET



2D ELITE code shows edge pressure gradient close to ballooning limit & predicts broad mode structures

[A. Kirk et al, EX/9-1]

UKAEA



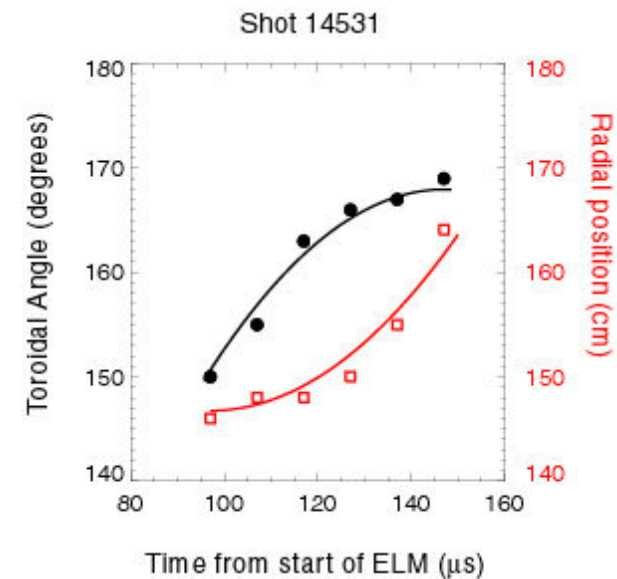
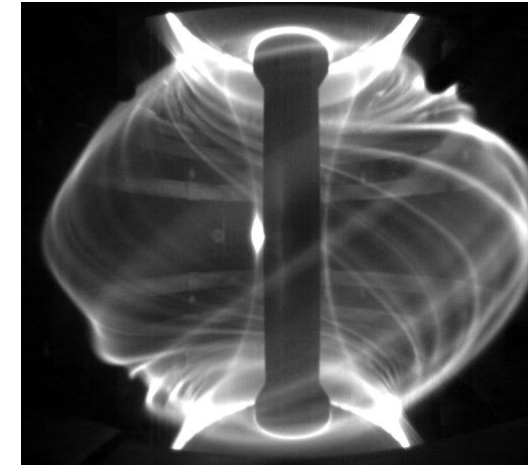


ELM Filaments

Type I ELM filaments exhibit the same characteristics at high and low collisionality

Analysis of high speed images (up to 200kHz) shows that the ELM filaments:

- are aligned with B
- have constant width
- toroidal mode number typically $n = 10 - 15$
- remain close to the LCFS for 50 - 100 μ s during which most of the energy & particle loss (50 -75%) occurs
- initially rotate toroidally with pedestal then decelerate toroidally and accelerate radially outwards



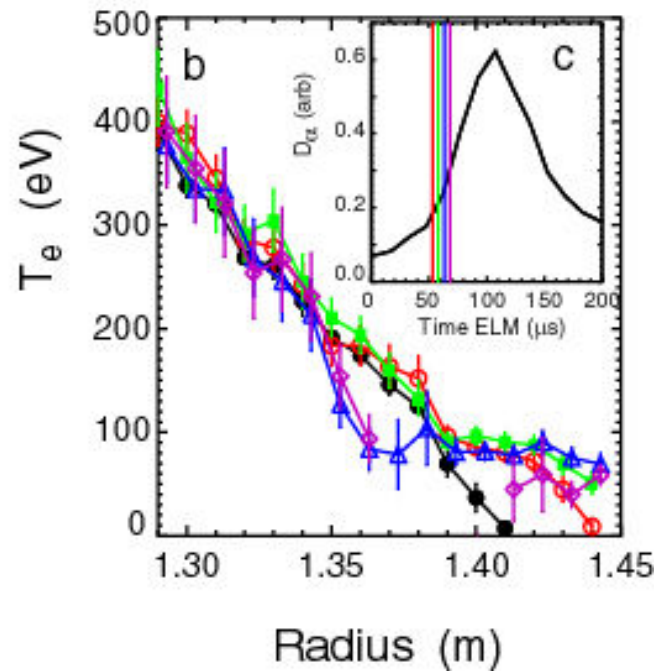
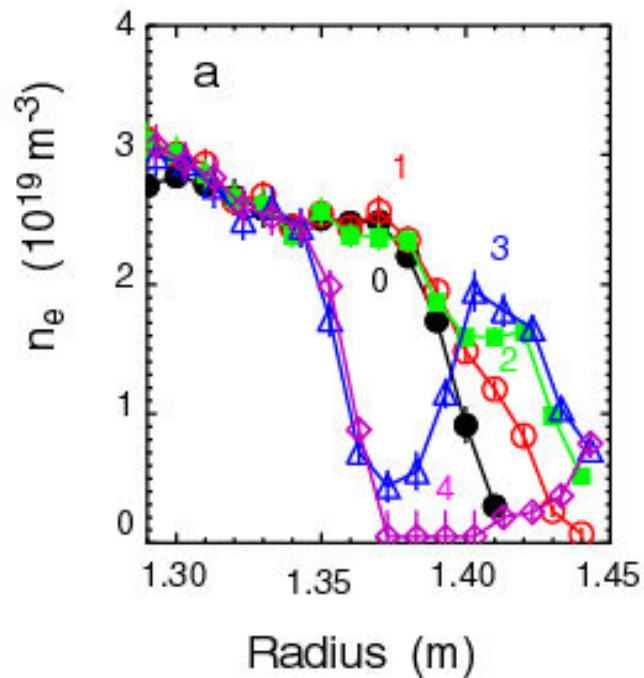
[A. Kirk et al, Phys. Rev. Lett. 96 (2006) 185001]



ELM filaments – energy content

Edge TS measurements of ELM filaments:

- confirm radial acceleration
- quantify energy & particle content ($< 2.5\%$ of ΔW_{ELM} per filament)

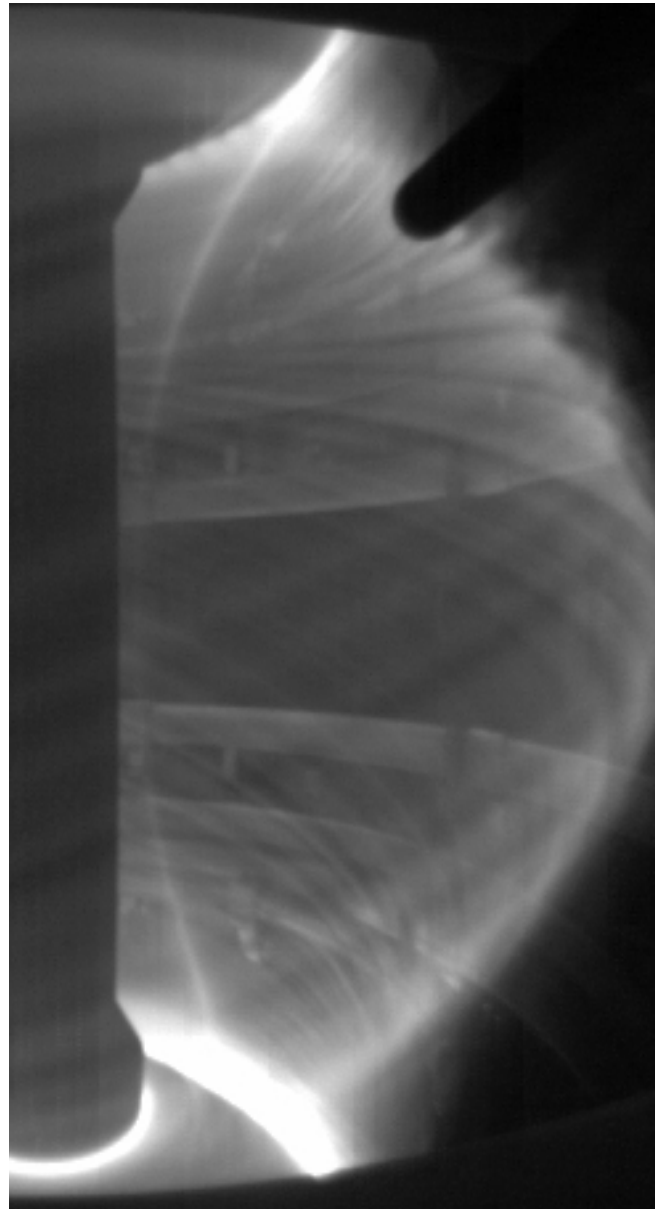


1cm spatial resolution
4 lasers fired with 5 μs
separation

[A. Kirk et al, EX/9-1]



Filamentary structures in MAST



UKAEA

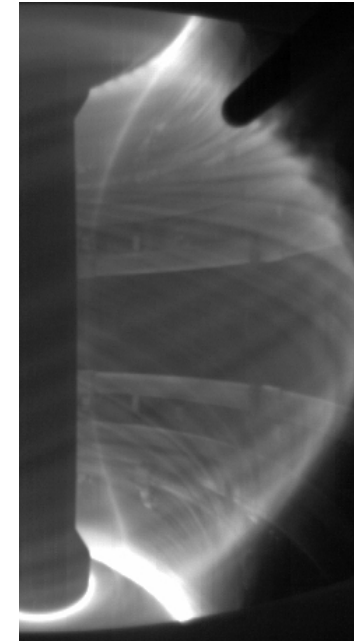




L-mode turbulence

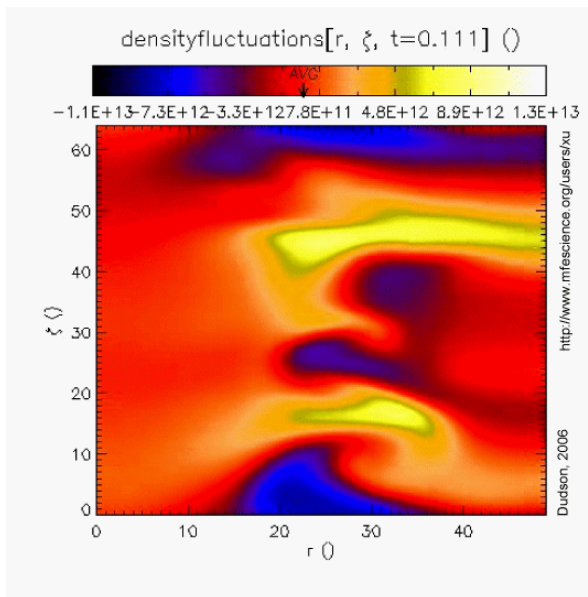
L-mode filaments:

- ❑ Correlated with intermittent bursts on probe data
- ❑ Aligned along B
- ❑ High toroidal mode number $n = 30 - 50$
- ❑ Constant toroidal & radial velocity
- ❑ Disperse/disintegrate as they move outwards



BOUT
(LLNL)

toroidal



radial

Powerful statistical techniques are being applied to probe data and BOUT output to identify similarities/differences in L-mode turbulence

Electrostatic drift wave turbulence and interchange-like instabilities may both play a role [G. Counsell et al, EX/P4-6]

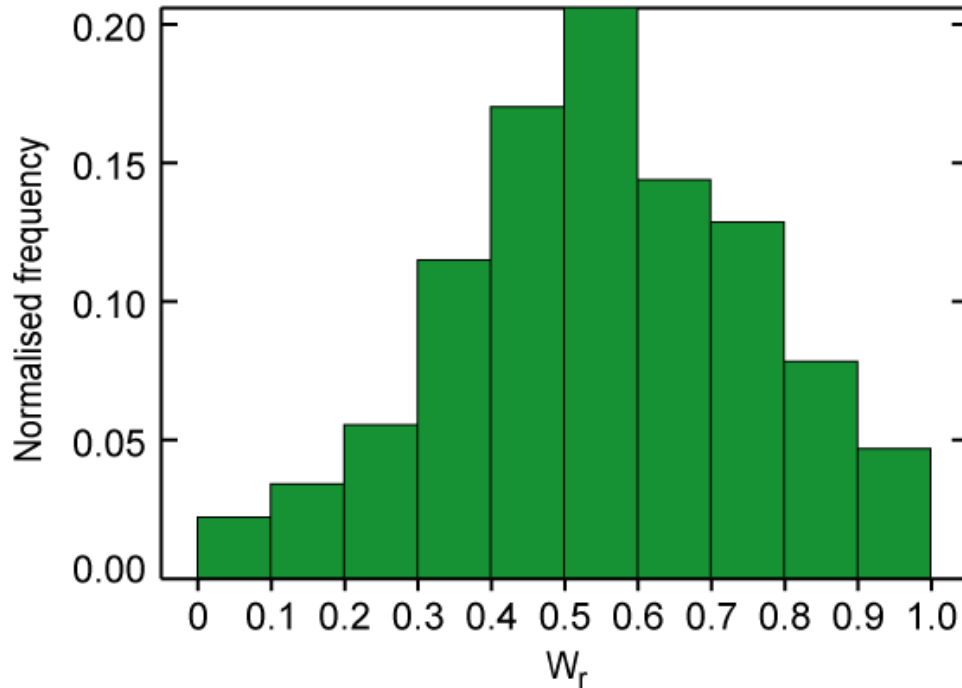
UKAEA





Disruption power loads

Significant loss of W_{th} prior to thermal quench in most MAST disruptions



Database of 1100 disruptions

$$W_r = W_{tq} / W_{tq-20ms}$$

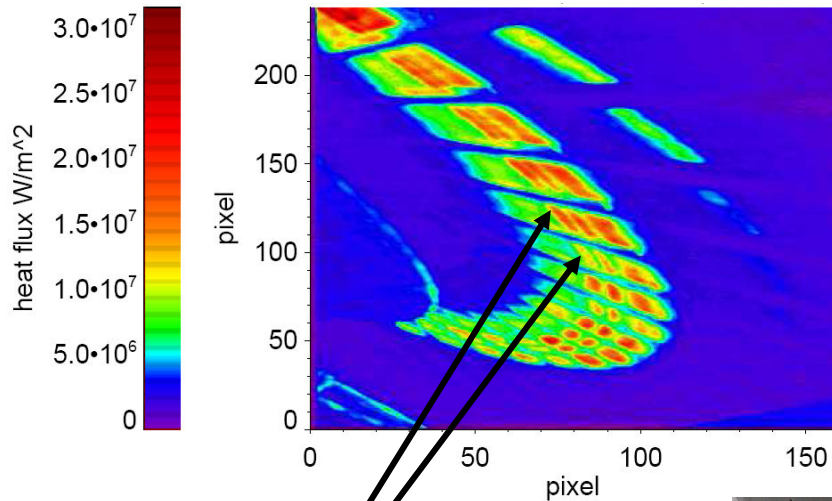
$$\langle W_r \rangle = 0.55 \pm 0.2$$

Peak divertor heat load during thermal quench also ameliorated due to x 5 - 9 increase in heat flux width Δ_h



Disruption power loads

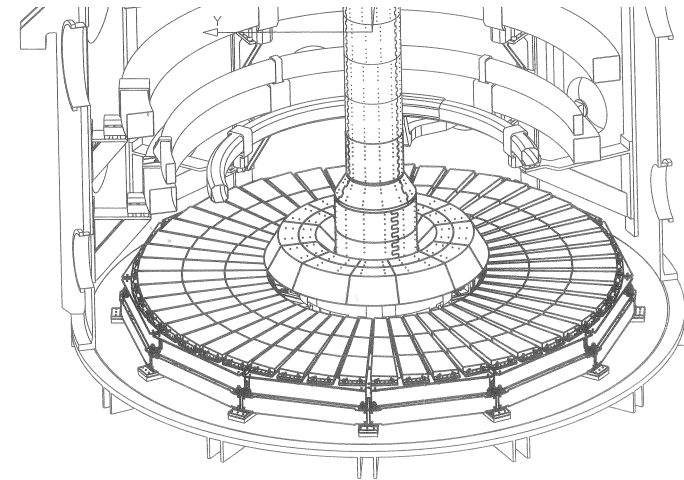
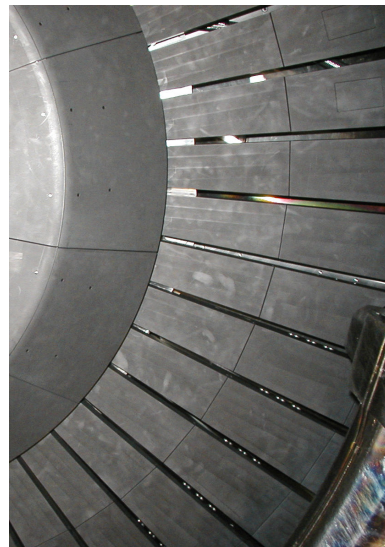
□ Spatial distribution of power loading is complex, e.g.



'Braiding' of strike points observed during disruptions triggered by a giant sawtooth

Locked mode disruptions typically exhibit double strike points

Note lack of toroidal symmetry – almost universally observed in MAST disruptions of all types





Summary

MAST is addressing a wide range of key physics issues for ITER and future STs, aided by increasingly powerful diagnostic capabilities and supported by theory and numerical modelling. Ongoing developments (e.g. to NBI and plasma control systems) are preparing the way for long pulse operation.

Related presentations

S.D. Pinches et al, “MHD studies in MAST” **EX/7-2Ra**

A. Kirk et al, “Evolution of the pedestal on MAST and the implications for ELM power loadings” **EX/9-1**

J.W. Connor et al, “Turbulent transport in spherical tokamaks with transport barriers” **TH/P2-2**

G.F. Counsell et al, “Analysis of L-mode turbulence in the MAST boundary plasma” **EX/P4-6**

R.J. Akers et al, “The influence of beam injection geometry upon transport and current drive in MAST” **EX/P3-13**

V. Shevchenko et al, “Electron Bernstein wave heating experiments on MAST” **EX/P6-22**

UKAEA

